ASSESSMENT OF LARGE EDDY SIMULATIONS FOR AGITATED FLOWS

J. DERKSEN

Kramers Laboratorium, Delft University of Technology, Delft, The Netherlands.

Large eddy simulations (LES) on the single-phase flow driven by a pitched blade impeller in a baffled stirred tank reactor were performed. The geometry, and operation conditions (defined in terms of $Re = 7,300$) were chosen to comply with the experimental work by Schäfer *et al*. As the turbulence in stirred tanks is strongly off-equilibrium, no straightforward criteria with respect to spatial and temporal resolution of the simulations can be formulated, and experimental validation becomes of prime importance. In this study, the influence of the resolution, and the specific choice of the subgrid-scale model (standard Smagorinsky model, and structure function model) on the simulated flow field were investigated.

Keywords: stirred tanks; turbulence; large eddy simulation; subgrid-scale models.

INTRODUCTION

In recent years, large eddy simulations (LES) of turbulent, single-phase flows have entered chemical engineering research. LES of agitated flow systems have been reported by Eggels[1], Revstedt *et al*.[2], Derksen and Van den Akker[3], and Bakker *et al*.[4]. The results with respect to the average flow fields, and fluctuating velocities are very promising. Moreover, LES provides detailed, time-dependent flow information. This information is very useful for including micro-scale physics and/or chemistry in the simulation procedure. For instance, the hydrodynamic conditions under which droplets in liquid-liquid dispersions break up or coalesce can be simulated in fairly great detail. In the field of crystallization, Hollander *et al*.[5] reported an LES based numerical study on agglomeration in stirred tanks. In combustion research, LES is nowadays applied extensively in combination with micro-mixing modelling[6].

The basic idea behind large eddy simulations is filtering[7]. In general, strongly turbulent flows cannot be fully resolved in a simulation due to the very wide range that exists between the largest and smallest (dissipative) scales. By means of low-pass filtering the Navier–Stokes equations, and setting up appropriate models for the subgrid-scale (SGS) terms that appear after the filter operation, the range of resolved scales is narrowed to a size that is tractable for numerical simulation. In case of homogeneous flows, clear rules exist with respect to the applicability and validity of SGS models. For instance, the Smagorinsky model[8] is based on equilibrium between production and dissipation in the inertial subrange. From this assumption, it immediately follows that the grid spacing in a numerical simulation should be such that at least part of the inertial subrange can be resolved. In stirred tanks, however, there will be hardly any position where equilibrium can be assumed.

Production of turbulence will mainly take place in the impeller swept volume, while a much larger part of the tank volume takes part in dissipation. Furthermore, due to the presence of an impeller revolving relative to a baffled tank wall, the flow is intrinsically unsteady. As a result, it is not an equilibrium flow.

The objections listed above have not kept away people from doing LES in complex flows, including stirred tanks. In view of the objections, however, a good assessment of the simulation results in terms of consistency and experimental validation is of prime importance. The influence of grid size has to be studied carefully, as the grid plays a more important role in an LES than in a RANS simulation. In the first place (just as in RANS simulations) it is the basis for discretization. Its second role is that of a low pass filter: fluctuations at SGS level are filtered out.

In this paper, results on the flow case defined experimentally by Schäfer *et al*.[9] will be presented. The case was chosen here because of the good quality of the experimental data available. The emphasis of the paper will be on the influence of the spatial resolution on the simulation results, and on comparing two SGS models, *viz* the standard Smagorinsky model, and the structure function model[10].

SIMULATION PROCEDURE

The simulation procedure that has been followed here has been documented in Derksen and Van den Akker[3]. As high spatial resolution is an important issue in LES of complex flows, an efficient flow solver based on lattice-Boltzmann discretization has been applied. The lattice-Boltzmann method is a relatively new type of time-dependent Navier–Stokes solver in the incompressible flow regime[11]. Unlike conventional CFD schemes based on the discretization of

the Navier–Stokes equation, the lattice-Boltzmann method is based on a kinetic model for the fluid. The model system consists of particles residing on a uniform (and in this case cubic) lattice. Every time step, the particles move to neighboring lattice sites where they exchange momentum (i.e. collide) with particles coming from other directions. With the appropriate choices for the collision rules and lattice symmetry properties, it can be proven that this discrete model represents the Navier–Stokes equation[12]. The method employs explicit time stepping, and has second order accuracy in space and time.

In Derksen and Van den Akker, the standard Smagorinsky model was used exclusively for SGS modelling. Recently a structure function model was implemented in the computer code.

Structure Function Subgrid-Scale Models

Structure function models[10] are (just as the Smagorinsky model) based on the eddy viscosity concept. They stem from Kraichnan's equation for the kinetic energy spectrum[13]. From this equation, energy transfer rates as a function of wave number can be estimated. This way, a wave number dependent eddy viscosity can be calculated. In the structure function model, these concepts are translated from wave number space to physical space. The structure function eddy viscosity (ν_e^{SF}) as a function of the position in space x, and grid spacing Δ then reads:

$$\nu_e^{SF}(x, \Delta) = 0.105 \, C_K^{-3/2} \Delta [F_2(x, \Delta)]^{1/2} \qquad (1)$$

with C_K a constant. The (second-order velocity) structure function F_2 is defined as:

$$F_2(x, \Delta) = \left\langle ||u(x, t) - u(x + r, t)||^2 \right\rangle_{||r = \Delta||} \qquad (2)$$

with u being the resolved velocity field. The averaging, denoted by $\langle \rangle$, is over the six closest grid nodes.

Due to the uniformity of the computational grid, the six nearest neighbours all have the same distance to the point under consideration. The constant C_K was estimated to be 1.4 in case of isotropic turbulence[7].

In the case where the differences between neighbouring velocity values in the structure function equation (2) are approximated in terms of spatial derivatives, and C_K amounts to 1.4, the structure function eddy viscosity takes a form similar to the eddy viscosity as it emerges from the Smagorinsky model:

$$\nu_e^{SF} \approx 0.77 (c_s \Delta)^2 \sqrt{2 S_{ij} S_{ij} + \omega_i \omega_i} \qquad (3)$$

with c_s the Smagorinsky constant[8], S_{ij} the resolved deformation tensor, and ω_i the resolved vorticity. The Smagorinsky model reads:

$$\nu_e^{Sm} = (c_s \Delta)^2 \sqrt{2 S_{ij} S_{ij}} \qquad (4)$$

As a consequence, in the absence of vorticity, the structure function model reduces to the Smagorinsky model, albeit with about 80% of its viscosity.

In shear flows, the value of the Smagorinsky constant c_s is generally taken close to 0.1[14]. The (ad hoc) reason for this is that applying the theoretical value of $c_s = 0.17$ (based on homogeneous, isotropic turbulence, and a lattice spacing such that wave number $k_\Delta = 2\pi/\Delta$ is lying in the inertial

subrange) to shear flows leads to too much damping. In this study, the value was taken as $c_s = 0.1$. For consistency, in the structure function model as approximated in equation (3) a value $c_s = 0.1$ was also assumed, implying that the constant C_K equation (1) was set to 3.0. This is approximately a factor of 2 larger than $C_K = 1.4$, which applies to homogeneous, isotropic turbulence.

Set-up of the Simulations

The stirred tank geometry is depicted in Figure 1. In the experimental work[9], the Reynolds number (defined as $Re = ND^2/\nu$, with N the angular velocity of the impeller (in rev s^{-1}), D the diameter of the impeller, and ν the kinematic viscosity of the fluid) was set to 7,300. A cubic computational domain, consisting of 120^3, 240^3, or 360^3 grid nodes was defined. Within this domain, the geometry of the tank and the (revolving) impeller were defined in terms of points on their surface. At these points, no slip boundary conditions were imposed by means of a dynamics, adaptive force-field technique[3]. The blade thickness (δ) was chosen to be an integer number times the lattice spacing: 0, 1, and 2 for the 120^3, 240^3, and 360^3 cases, respectively (i.e. $\delta = 0.0$, $0.013D$, and $0.017D$). In the experiment the blade thickness was $0.018D$.

The memory requirements of the lattice-Boltzmann code are perfectly linear with the number of lattice-sites. Per lattice-site, 21 four-byte real values need to be stored (one real for each velocity direction, and three force components). The largest simulations had grids of 360^3 (47 million) nodes. They used some 4 Gbyte of memory. The computer code was implemented on a Beowulf cluster consisting of 6 dual Pentium III machines running at 500 MHz, and connected through 100 BaseTX (100 Mbit/s) switched Ethernet. It was explicitly decided to develop and run the simulations on relatively cheap, pc-based computer hardware. This way, a potential obstacle for industrial application of the methodology can be overcome, as running the code does not require large costs in hardware and maintenance. The local nature of the operations involved in the lattice-Boltzmann scheme makes it well suited for distributed memory computing.
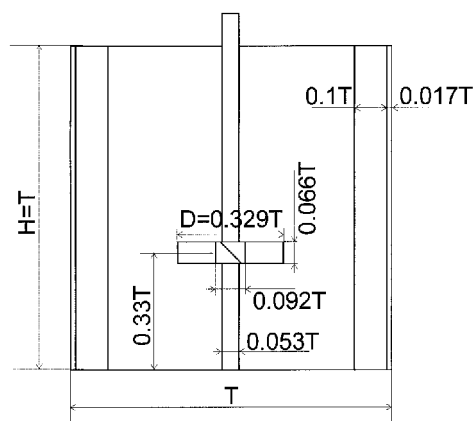
Figure 1. Stirred tank geometry. The tank has four, 90° spaced baffles, with a small wall clearance. The impeller has four pitched blades under a 45° angle. The top surface is closed.

The code was written in Fortran77. MPI was used for message passing. The wall-clock time to simulate a single impeller revolution on the largest grid with the code running on 9 processing elements (PE's) amounted to 44 hours. The wall-clock time was almost perfectly inversely linear proportional to the number of processing elements (a speed-up of 8.9 on 9 PE's), and linear proportional to the number of lattice sites used in the simulation.

The explicit nature of time-stepping in the lattice-Boltzmann method implies that the size of the time step is related to the lattice spacing. A single impeller revolution is 1,500 time steps on the 120^3 grid, 2,800 on the 240^3 grid, and 4,200 on the 360^3 grid. The statistical data (e.g. average velocities, and Reynolds stresses) of the various simulation cases were gathered over runs of at least 15 impeller revolutions, except for the simulation on the 360^3 grid that (due to the high computational effort) only extended over 6 impeller revolutions. Before starting to gather flow data for statistical processing, the (running averaged) flow field was monitored in order to ensure that a quasi steady state had been reached. Only the coarsest simulations were started from rest. The starting fields of the other simulations were interpolated from a coarser simulation that had reached steady state.

RESULTS

Figure 2 presents typical simulation results. The instantaneous realization of the flow (left-side vector plot) clearly shows the action of the impeller, and the vortical structures associated with it. A large quiescent volume can be identified in the top half of the tank. Due to the relatively low Reynolds number, fluid is forced upward along the baffled tank wall only to a limited extend[15]. The latter effect is also observed in the time averaged flow field (right side of Figure 2). The dominant flow feature here is a large circulation loop; downward flow near the axis, upward flow near the tank wall. On average, a secondary circulation can be observed near the corner formed by the tank bottom and the axis.

In comparing the LES results with experimental data, the authors first focussed on the global, phase averaged flow

V_{tip} ◁—   ◁— V_{tip}
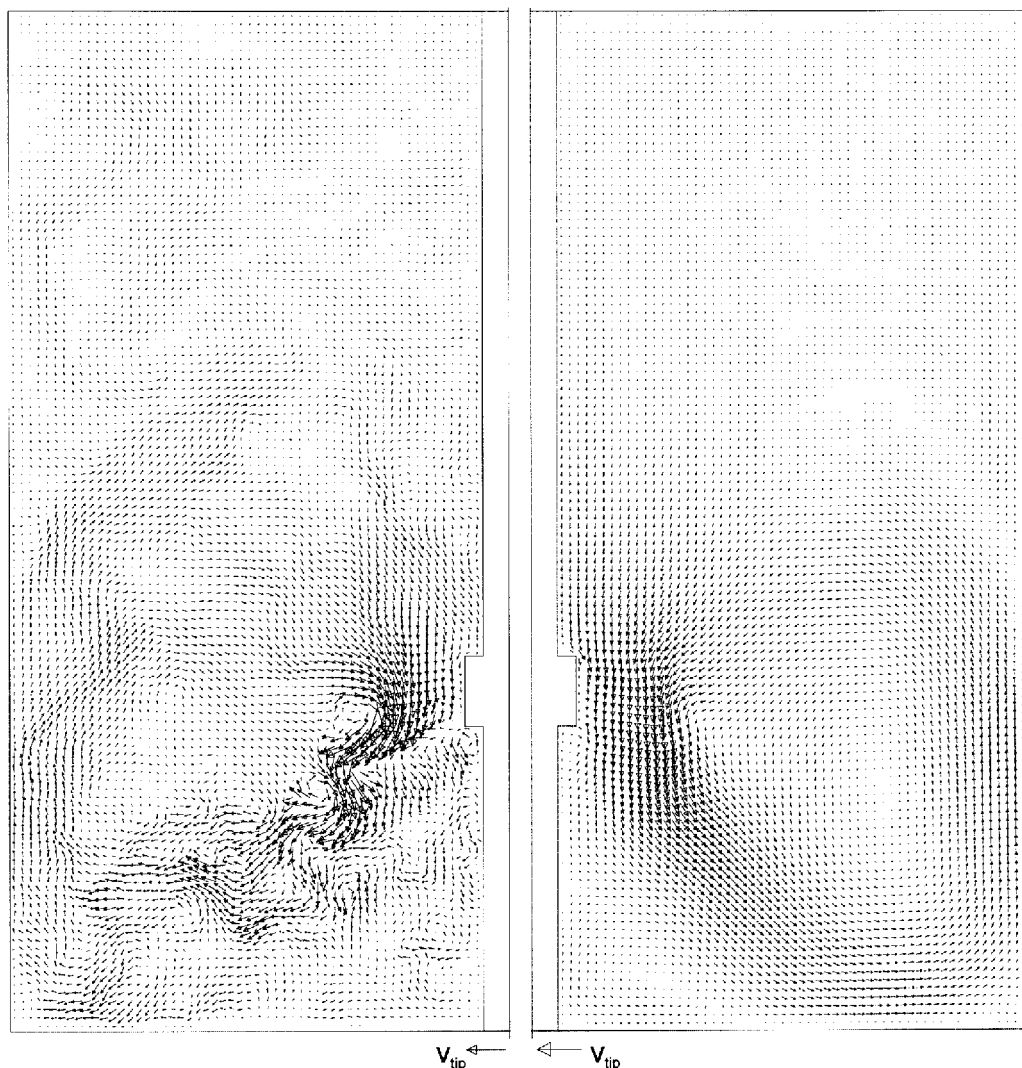
Figure 2. Single realization (left) and time-averaged flow (right) of the flow in a vertical plane midway between two baffles in terms of velocity vectors. The spatial resolution of the vector plots is (in axial *and* radial direction) twice as low as the actual resolution of the simulation.

field. In the entire vertical plane, midway between two baffles, velocities have been measured in a finely spaced grid by Schäfer et al.[9], see Figure 3(a). The average upward flow close to the tank wall only extends over a limited axial distance. At $z/T = 0.49$ (with z the distance from the bottom, and T the tank height), the axial velocity component in the column of measurement points closest to the wall changes sign. A secondary recirculation in the corner close to the axis and bottom already observed in Figure 2 is also present in the experiment. Figures 3(b)–(e) show results of large eddy simulations on grids with different spatial resolutions and/or SGS models. The simulation on the coarsest grid shows the strongest deviation from experimental data. The location of the main circulation is predicted at a too high axial position, and a too low radial position. Furthermore, the upflow underneath the impeller, near the axis extends over the full impeller bottom clearance, whereas in the experiment it is present between $z/T = 0$, and $z/T = 0.096$. The quality of the predictions improves significantly if the grid is refined. The simulation on the 360^3 grid (see Figure 3(e)) shows good correspondence with respect to the location of the main circulation centre, as well as the size of the secondary recirculation in the lower left corner. The strongest deviation observed is the too limited extent of the upflow near the tank wall: at $z/T = 0.42$ the axial velocity changes sign (the experimental value was 0.49). This position is known to be very sensitive to the Reynolds number[15]. In the simulations done by Wechsler et al.[16] an identical flow geometry was chosen. The Reynolds number, however, amounted to 29,000. As a result, the upflow near the tank wall was strongly overpredicted. The authors speculate that an extension of the Smagorinsky model with wall damping functions will improve the predictions (Derksen and Van de Akker[17] demonstrated that wall damping significantly improved the quality of LES on swirling flows in cyclones). As a final remark concerning Figure 3(e), the relatively strong, erratic flow in the upper part of the tank, is highlighted. This is due to the limited temporal extent of the simulations: only six impeller revolutions have been simulated.

Figures 3(c) and 3(d) are the result of simulations on a 240^3 grid. The difference between the two vector plots is the SGS model. Figure 3(c) relates to the Smagorinsky model,
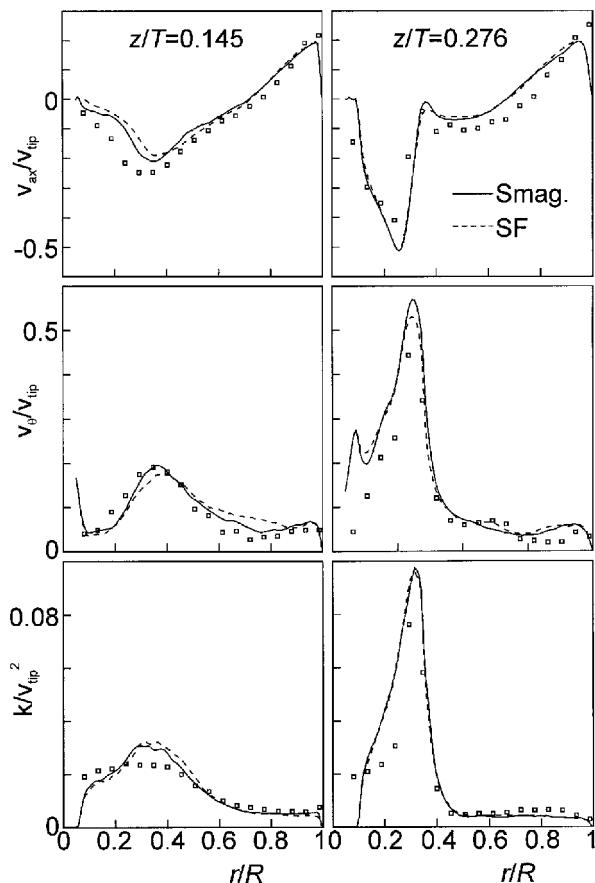
Figure 4. Phase-averaged profiles of the axial velocity (top), tangential velocity (middle), and turbulent kinetic energy (bottom) as a function of the radial position at two different axial levels in the tank: $z/T = 0.145$ (left), and $z/T = 0.276$ (right), in the vertical plane midway between two baffles. Comparison between experiment (symbols), and LES on a 240^3 grid with two different SGS models (*viz* the Smagorinsky model, and the structure function model).
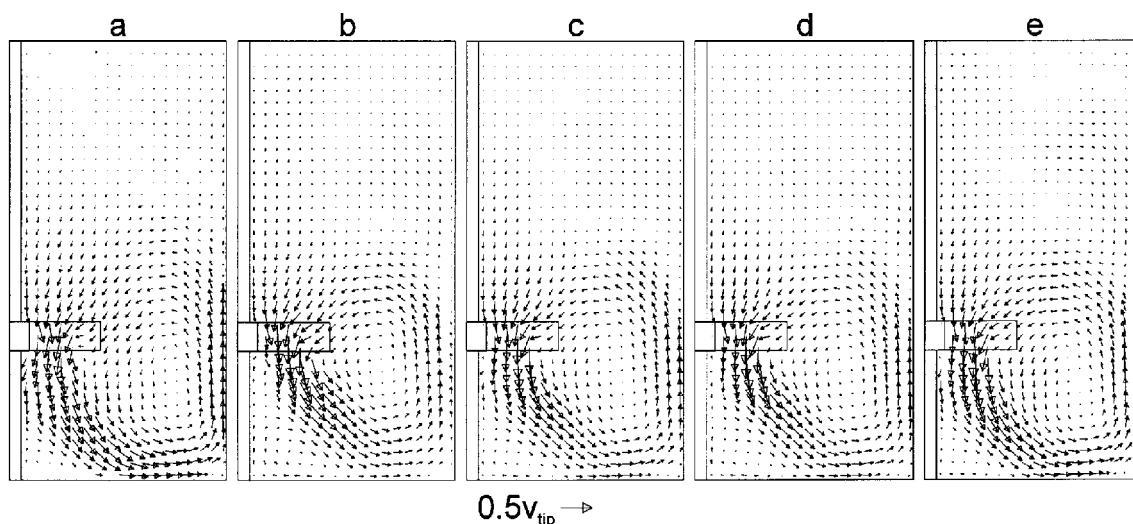
Figure 3. Phase-averaged velocity fields in the vertical plane midway between two baffles. (a) Experimental data[9]; (b) 120^3 grid, Smagorinsky model; (c) 240^3 grid, Smagorinsky model; (d) 240^3 grid, structure function model; (e) 360^3 grid, Smagorinsky model. The simulation results have been linearly interpolated to the experimental grid.

whereas Figure 3(d) relates to the structure function model. No significant differences between the two results can be observed. There are some small (but significant) differences between the 240^3 cases, and the 360^3 case. The radial position of the main circulation is slightly more inwards for the 240^3 case. Furthermore, the lower left corner recirculation is a little bigger. These two effects demonstrate the demand for highly resolved simulations.

In Figure 4, the predictions made by the Smagorinsky model are compared with those of the structure function model in terms of phase-averaged radial profiles. Also in this perspective, not much difference between the results of the two SGS models can be observed. Axial velocities are predicted fairly accurately. The deviations already observed in the vector plots are apparent in the profiles. The radial

position where the simulated profiles at $z/T = 0.276$ cross the zero level is too far to the left, demonstrating that the centre of the main circulation is at a too small radius. The tangential velocity profile at $z/T = 0.276$ shows a secondary peak not observed in the experiment. The predicted turbulent kinetic energy levels are in accordance with the experimental data. As has been demonstrated before[3], LES does a better job than RANS simulations in predicting kinetic energy levels in stirred tanks (compare the present results with the ones obtained by Syrjänen and Manninen[18]).

Phase-resolved vector fields in the vicinity of the impeller reveal the tip vortex formation. The position, size, and shape (squeezed for small angles, circular for larger angles) are well represented by the simulations (see Figure 5). Here it is possible to observe some significant differences between the
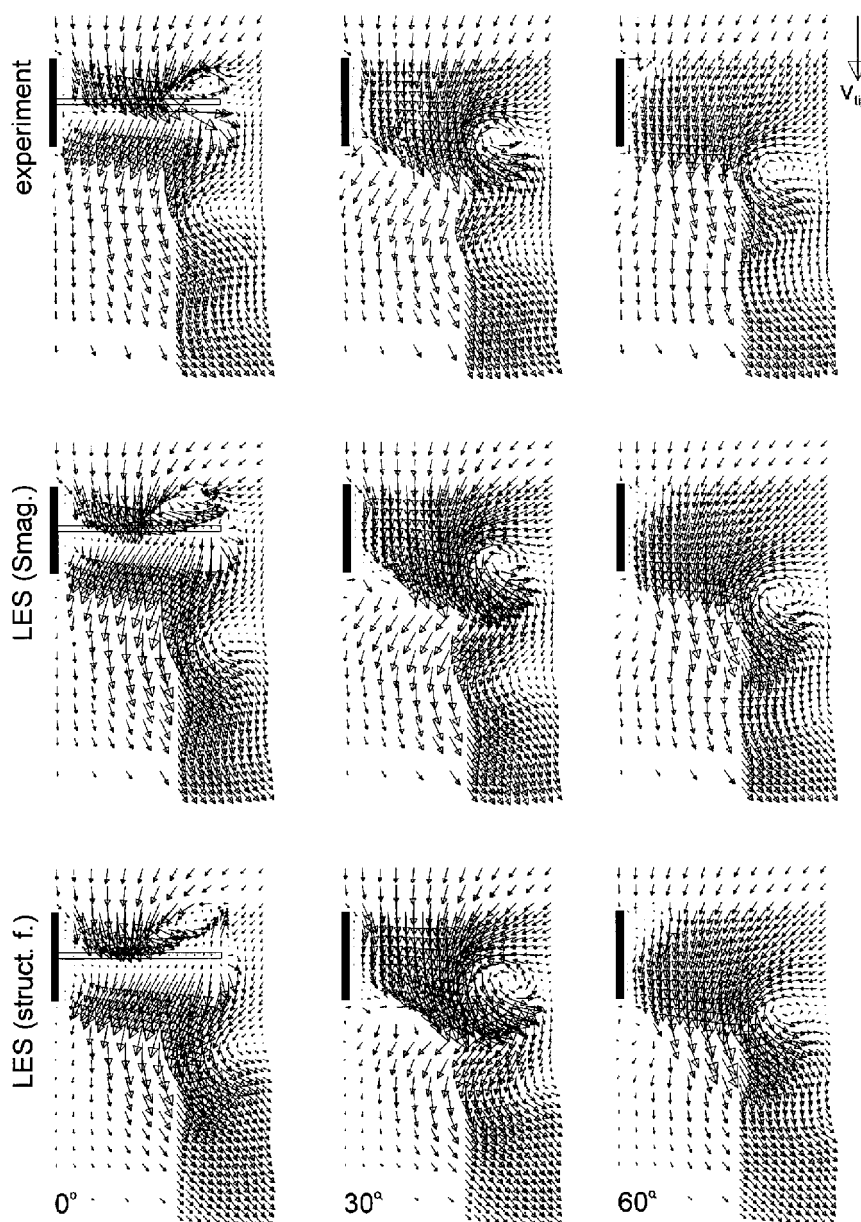
Figure 5. Phase-resolved velocity fields in the vicinity of the impeller, in a vertical plane midway between two baffles, at three angular positions of the impeller: 0°, 30°, 60°. The location of the impeller is indicated in the 0° plots. The upper row represents experimental data, the middle row LES on a 240^3 grid with the Smagorinsky model, the lower row LES on a 240^3 grid with the structure function model.
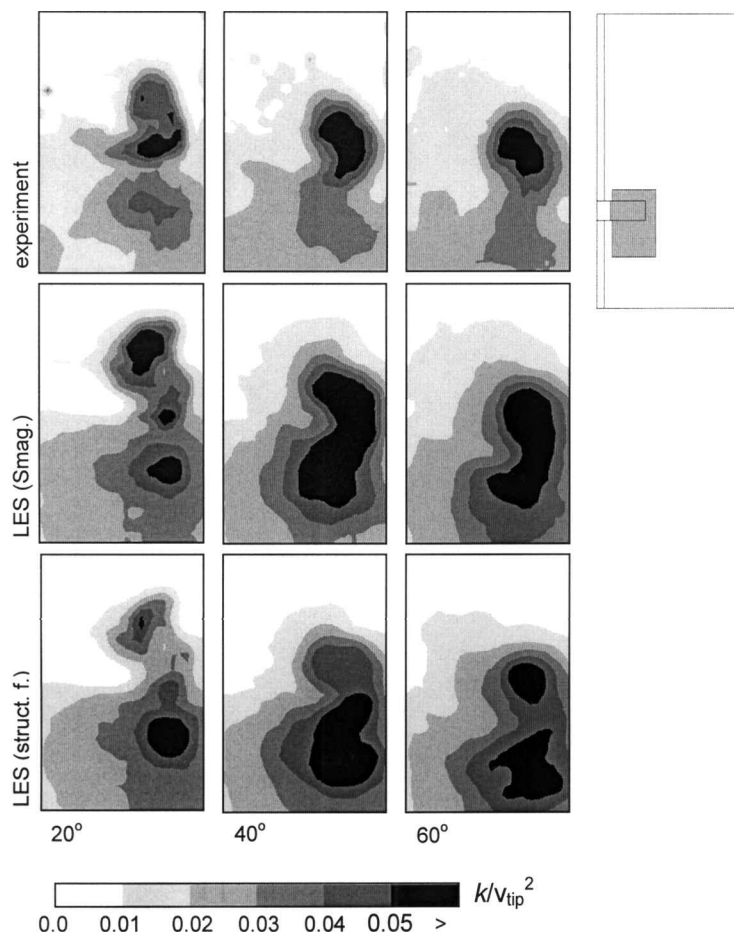
Figure 6. Phase-resolved contour plots at three different impeller angles of the turbulent kinetic energy in the vicinity of the pitched blade turbine (the field of view is indicated in the right diagram). Top row: experiments. Middle row: LES on a 240^3 grid with use of the Smagorinsky model. Lower row: LES on a 240^3 grid with the structure function model.

predictions obtained with the Smagorinsky model, and the structure function model: the initial strength of the tip vortex (i.e. at zero angle position) is less in the case of the structure function model. This may be related to the eddy viscosity being strongly dependent on the vorticity in the case of the structure function model (see equation (3)). As a consequence, more damping is introduced in regions with strong vorticity. If the two predictions at zero angle impeller position are compared with the experimental evidence, the Smagorinsky model appears to perform better, although the velocity levels directly underneath the vortex are overpredicted. For the two other angular position depicted in Figure 5 (30° and 60°), predictions with the two SGS models do not show noticeable differences.

Phase-resolved turbulent kinetic energy predictions can be found in Figure 6. In the near wake of the blade (at 20°), the experiment shows three spots of relatively strong turbulent activity (i.e. high k): the top spot can be associated with the freshly formed tip vortex, the middle spot lies in the vicinity of the blade tip, and bottom spot is related to the vortex generated during the previous blade passage. In the Smagorinsky model predictions, these spots can also be observed, albeit with different (relative) strength. The structure function predictions hardly show the spot near the blade tip. At higher angular values, the spots in the experiment appear to merge. This is also the case for the predictions

obtained with the Smagorinsky model. The levels of kinetic energy are, however, approximately 20% too high. The structure function model shows a different picture. Here, the turbulent kinetic energy in the vortex core seems to increase at increasing angular position of the impeller. The mechanism (in terms of the SGS modelling assumptions) for this is not clear yet. What is clear, is that it does not fully correspond to the experimental findings.

CONCLUSIONS

Results of large-eddy simulations (LES) of the flow driven by a pitched blade turbine have been presented. It was demonstrated that the spatial resolution has a significant impact on the overall average flow field results. A 360^3 mesh showed the best agreement with experimental data. The impact of a slightly different subgrid-scale (SGS) model (a structure function model instead of a Smagorinsky model) did not lead to significant changes in the overall, phase-averaged flow field results.

The phase-resolved velocity field in the vicinity of the impeller was well represented by the simulations. The formation, and strength of the tip vortex differed for the two SGS approaches: the vortex formed in the structure function simulations was weaker. The levels of (phase-resolved) kinetic energy were overpredicted by some 20%

by the Smagorinsky model. This is in remarkable contrast to RANS simulations that usually underpredict kinetic energy levels. The structure function predictions show a rather late (in terms of angular position of the impeller) development of a high kinetic energy region that coincides with the vortex core.

REFERENCES

1. Eggels, J. G. M., 1996, Direct and large-eddy simulations of turbulent fluid flow using the lattice-Boltzmann scheme, *Int J Heat Fluid Flow*, 17: 307.
2. Revstedt, J., Fuchs, L. and Trägårdh, C., 1998, Large eddy simulations of the turbulent flow in a stirred tank reactor, *Chem Eng Sci*, 53: 4041.
3. Derksen, J. J. and Van den Akker, H. E. A., 1999, Large eddy simulations on the flow driven by a Rushton turbine, *AIChE J*, 45(2): 209.
4. Bakker, A., Oshinowo, L. and Marshall, E. M., 2000, The use of large eddy simulations to study stirred vessel hydrodynamics, *Proc 10th Europ Conf Mixing* (Elsevier, Amsterdam), pp 247.
5. Hollander, E. D., Derksen, J. J., Bruinsma, O. S. L., Van Rosmalen, G. M. and Van den Akker, H. E. A., 2000, A numerical investigation into the influence of mixing on orthokinetic agglomeration, *Proc 10th Europ Conf Mixing* (Elsevier, Amsterdam), pp 221.
6. Colucci, P. J., Jaberi, F. A., Givi, P. and Pope, S. B., 1998, Filtered density function for large eddy simulation of turbulent reacting flows, *Physics of Fluids*, 10: 499.
7. Lesieur, M. and Métais, O., 1996, New trends in large eddy simulation of turbulence, *Annu Rev Fluid Mech*, 28: 45.
8. Smagorinsky, J., 1963, General circulation experiments with the primitive equations: 1. The basic experiment, *Mon Weather Rev*, 91: 99.
9. Schäfer, M., Yianneskis, M., Wächter, P. and Durst, F., 1998, Trailing vortices around a 45° pitched-blade impeller, *AIChE J*, 44: 1233.
10. Métais, O. and Lesieur, M., 1992, Spectral large eddy simulations of isotropic and stably stratified turbulence, *J Fluid Mech*, 239: 157.
11. Frisch, U., Hasslacher, B. and Pomeau, Y., 1986, Lattice-gas automata for the Navier–Stokes equations, *Phys Rev Lett*, 56: 1505.
12. Chen, S. and Doolen, G., 1998, Lattice-Boltzmann method for fluid flows, *Annu Rev Fluid Mech*, 30: 329.
13. Kraichnan, R. H., 1976, Eddy viscosity in two and three dimensions, *J Atoms Sci*, 33: 1521.
14. Moin, P. and Kim, J., 1982, Numerical investigation of turbulent channel flow, *J Fluid Mech*, 118: 341.
15. Bittorf, K. J. and Kresta, S. M., 2000, Limits of fully turbulent flow in a stirred tank, *Proc 10th Europ Conf Mixing* (Elsevier, Amsterdam), pp 17.
16. Wechsler, K., Breuer, M. and Durst, F., 1999, Steady and unsteady computations of turbulent flows induced by a 4/45° pitched-blade impeller, *J Fluids Eng*, 121: 318.
17. Derksen, J. J. and Van den Akker, H. E. A., 2000, Simulation of vortex core precession in a reverse-flow cyclone, *AIChE J*, 46: 1317.
18. Syrjänen, J. K. and Manninen, M. T., 2000, Detailed CFD prediction of flow around a 45° pitched blade turbine, *Proc 10th Europ Conf Mixing* (Elsevier, Amsterdam), pp 255.

ADDRESS

Correspondence concerning this paper should be addressed to J. Derksen, Kramers Laboratorium, Delft University of Technology, Prins Bernhardlaan 6, 2628 BW Delft, The Netherlands.
E-mail: jos@klft.tn.tudelft.nl